Original article

MOLECULAR METABOLISM

Leptin receptor neurons in the dorsomedial hypothalamus are key regulators of energy expenditure and body weight, but not food intake

Kavon Rezai-Zadeh [1], Sanghou Yu [1], Yanyan Jiang [2], Amanda Laque [1], Candice Schwartzenburg [1], Christopher D. Morrison [3], Andrei V. Derbenev [2], Andrea Zsombok [2], Heike Münzberg [1,*]

ABSTRACT

Objective: Leptin responsive neurons play an important role in energy homeostasis, controlling specific autonomic, behavioral, and neuroendocrine functions. We have previously identified a population of leptin receptor (LepRb) expressing neurons within the dorsomedial hypothalamus/dorsal hypothalamic area (DMH/DHA) which are related to neuronal circuits that control brown adipose tissue (BAT) thermogenesis. Intra-DMH leptin injections also activate sympathetic outflow to BAT, but whether such effects are mediated directly via DMH/DHA LepRb neurons and whether this is physiologically relevant for whole body energy expenditure and body weight regulation has yet to be determined.
Methods: We used pharmacosynthetic receptors (DREADDs) to selectively activate DMH/DHA LepRb neurons. We further deleted LepRb with virally driven cre-recombinase from DMH/DHA neurons and determined the physiological importance of DMH/DHA LepRb neurons in whole body energy homeostasis.
Results: Neuronal activation of DMH/DHA LepRb neurons with DREADDs promoted BAT thermogenesis and locomotor activity, which robustly induced energy expenditure ($p < 0.001$) and decreases body weight ($p < 0.001$). Similarly, intra-DMH/DHA leptin injections normalized hypothermia and attenuated body weight gain in leptin-deficient *ob/ob* mice. Conversely, ablation of LepRb from DMH/DHA neurons remarkably drives weight gain ($p < 0.001$) by reducing energy expenditure ($p < 0.001$) and locomotor activity ($p < 0.001$). The observed changes in body weight were largely independent of food intake.
Conclusion: Taken together, our data highlight that DMH/DHA LepRb neurons are sufficient and necessary to regulate energy expenditure and body weight.

Keywords Leptin; Thermoregulation; Energy expenditure; Dorsomedial hypothalamus; DREADD

1. INTRODUCTION

Leptin regulates energy homeostasis by activating thermoregulatory responses, particularly brown adipose tissue (BAT) thermogenesis (also referred to as nonshivering thermogenesis). The importance of leptin-stimulated BAT thermogenesis has been well documented in rodent models [1–3]. For example, leptin-deficient mice are hypothermic and cold sensitive due to defects in BAT function [4–6]. Leptin also induces weight loss independent of food intake, via mechanisms that require functional BAT thermogenesis [7], suggesting that food-independent body weight control by leptin is mediated via BAT thermogenesis. Leptin treatment in obese humans is largely ineffective for reducing body weight [8], due to the common development of leptin resistance [9], but leptin's effect on energy expenditure has been demonstrated in weight-reduced and leptin-deficient humans where it prevents the drop in energy expenditure that is commonly associated with dieting [10,11]. Thus, the neuronal circuits that mediate leptin-stimulated BAT thermogenesis and energy expenditure hold promise as potential obesity therapy and warrant further investigation.

Despite the initial controversy surrounding the importance of BAT thermogenesis in adult humans and the control of body weight, thermogenic active BAT in adult humans is now well acknowledged and BAT size has been found to correlate negatively with body mass index [12,13]. BAT thermogenesis is governed by central mechanisms via the sympathetic nervous system [14,15], but the neuronal circuits that integrate specific peripheral signals into thermoregulatory responses are not entirely understood. Neuroanatomical and pharmacological approaches have identified several brain sites, including the dorsomedial hypothalamus/dorsal hypothalamic area (DMH/DHA), as key players in the control of BAT thermogenesis in rodents [14,16,17],

[1]Central Leptin Signaling, Pennington Biomedical Research Center (PBRC), LSU System, Baton Rouge, LA, USA [2]Department of Physiology, School of Medicine, Tulane University, New Orleans, LA, USA [3]Neurosignaling, Pennington Biomedical Research Center (PBRC), LSU System, Baton Rouge, LA, USA

*Corresponding author. Pennington Biomedical Research Center, Louisiana State University System, 6400 Perkins Rd, Baton Rouge, LA 70808, USA. Tel.: +1 225 763 2769; fax: +1 225 763 0260. E-mail: Heike.Munzberg@pbrc.edu (H. Münzberg).

Received July 16, 2014 • Revision received July 22, 2014 • Accepted July 25, 2014 • Available online 6 August 2014

http://dx.doi.org/10.1016/j.molmet.2014.07.008

but their role in body weight control has not been studied. We recently reported that BAT-related neurons in the DMH/DHA express leptin receptors (LepRb) and are activated by cold-exposure. Similar to cold- and pyrogen stimulated thermogenic pathways, DMH/DHA LepRb neurons innervate premotor neurons in the raphe pallidus (RPa) that control BAT thermogenesis [18]. Intra-DMH leptin activates sympathetic BAT inputs, but if this effect is indeed mediated directly by DMH/DHA LepRb neurons and if they contribute to whole body energy homeostasis remains unknown [19]. In this study we tested if DMH/DHA LepRb neurons are necessary and sufficient to promote BAT thermogenesis, energy expenditure, and body weight maintenance in mice.

2. METHODS

2.1. Mice

$LepRb^{GFP}$, $LepRb^{cre}$ (kindly provided by Dr. Martin Myers, Jr, University of Michigan, Ann Arbor, Michigan) and $LepRb^{fl/fl}$ mice (kindly provided by Dr. Streamson Chua, Jr, Albert Einstein College of Medicine, New York, New York) were bred in house from homozygous breeding pairs of $LepRb^{cre/cre}$, $Gt(ROSA)26Sor^{tm2Sho/tm2Sho}$, $LepRb^{cre/cre}$ mice, or $LepRb^{fl/fl}$ mice, respectively, and have been described in detail elsewhere [20–22]. Leptin-deficient *ob/ob* mice and their wildtype littermates (*+/?*) were purchased from the Jackson Laboratories (Bar Harbor, ME). All experiments were gender balanced, when both male and female mice were employed, and all animals were group housed at 22 °C–24 °C, maintained on a 12-h light/12-h dark cycle, and given *ad libitum* access to standard mouse chow and water unless stated otherwise. All animal experiments were approved by the institutional animal care and use committee.

2.2. Peripheral leptin treatment

Leptin was obtained from Dr. Parlow (National Hormone and Peptide Program, http://www.humc.edu/hormones). To identify LepRb neurons via leptin-induced pSTAT3, mice were injected intraperitoneally (i.p.) with leptin (5 mg/kg body weight) and perfused after one hour of incubation. For studies investigating leptin-induced cFos (as a surrogate of neuronal activity) in LepRb neurons, $LepRb^{GFP}$ mice were injected with vehicle (saline) or leptin (5 mg/kg, i.p.) and perfused three hours later.

2.3. Stereotaxic injection of adeno-associated viruses (AAVs) in the DMH/DHA

We used *designer-receptors-exclusively activated-by-designer drugs* (DREADD) technology to allow neuron-specific activation of DMH/DHA LepRb neurons. For DMH/DHA specific deletion of LepRb we injected a *cre*-expressing AAV or control virus into $LepRb^{fl/fl}$ mice. AAV-hSyn-DIO-hM3D(G_q)-mCherry (AAV-DREADD, kindly made available from Dr. Bryan Roth) and AAV-CMV-TR-EGFP (control virus) were obtained from the vector core of the University of North Carolina at Chapel Hill. AAV-CMV-HI-GFP-Cre-WPRE-SV40 virus (AAV-cre) was obtained from the vector core of the University of Pennsylvania. Three separate cohorts of $LepRb^{cre}$ mice (Group A–C) were used for AAV-DREADD injections targeted to the DMH/DHA as described earlier [23]. Two cohorts of $LepRb^{fl/fl}$ mice received control or AAV-cre virus injections targeted to the DMH/DHA. Mice were anesthetized with 5% isofluorane and their heads immobilized within the frame of a stereotaxic instrument (M1900 Stereotaxic alignment system; David Kopf Instruments, Tujunga, CA). Following sterilization of the surgical site, anesthesia was maintained at 1% isofluorane and an incision was made to expose the skull. Injections were aimed at −1.7 mm posterior, ±0.25 mm lateral and −4.6 mm ventral to Bregma according to the Paxinos Mouse Brain Atlas [24], and adjusted in $LepRb^{cre}$ mice to −1.1 mm posterior, ±0.25 mm lateral and −5 mm ventral to Bregma. Access holes were drilled and a bilateral guide cannula (Plastics One C253, Roanoke, VA) was inserted into the brain. A bilateral injector filled with virus (3–6 × 1012 viral molecules/ml) and attached to a 0.5 μl Hamilton syringe (Hamilton Company, Reno, NV) was threaded into the guide cannula and a volume of 200 nl per site was slowly infused into the DMH/DHA tissue at a rate of 20 nl per minute. Subsequently, the guide cannula and injector were removed, the skull access sealed with bone wax, and the incision closed with wound clips. Analgesics were applied once to the incision site (bupivacaine/lidocaine, 5 mg/kg) and subcutaneously during recovery every 12 h for two days (carprofen, 5–10 mg/kg). After the surgery mice were single housed for up to three weeks to allow for recovery and viral expression before further experimentation. Cannula placement and viral spread was verified histochemically at the end of all experiments.

2.4. Chronic intra-DMH/DHA cannulations for central leptin treatment

For DMH/DHA specific leptin or vehicle injections we chronically implanted bilateral cannulas (Plastics One C353, Roanoke, VA), as described in detail earlier [25], into the DMH/DHA. Briefly, procedures were identical to acute AAV injections, described above, but the bilateral guide cannula was secured in place with Loctite 454 (Fisher, Pittsburgh, PA) and dental cement before the incision was closed with wound clips. A dummy was inserted into the guide cannula to prevent contamination or blockage. Analgesics were applied as described above. Mice were allowed to recover for one week after surgery and adjusted to handling, twice daily saline injections, and body weight, food intake, and rectal temperature measurements over five days prior to leptin treatment to minimize stress. Body weight, food intake, and rectal temperature data were collected once per day prior to the second daily injection. After three consecutive days of leptin treatment, all mice were perfused and their brains were analyzed to confirm correct cannula placement.

2.5. Measurement of body temperature, energy expenditure, activity, body weight, and food intake in AAV-DREADD mice

Two cohorts of AAV-DREADD mice (group A, $n = 4$ and group B, $n = 4$) were injected once with the designer drug clozapine N-oxide (CNO, 0.3 mg/kg body weight; Sigma–Aldrich, St. Louis, MO) and rectal temperature was measured every 15 min for 90 min. In addition, two AAV-DREADD mice (from group B) were equipped with subcutaneous temperature transmitters (G2 E-Mitter; Respironics, Murrysville, PA). Temperature was continuously recorded in these two animals over three days of twice daily i.p. vehicle (saline) injections followed by three days of twice daily CNO (1.5 mg/kg body weight). Another separate cohort of DREADD mice (group C, $n = 8$) were shaved from head to tail along their backs to allow for temperature monitoring with an infrared/thermal camera (SC5000; FLIR Inc., Wilsonville, OR). Thermal photographs were taken at 10 min intervals following a single injection of vehicle or CNO (i.p., 1.5 mg/kg body weight). Two regions of interest (ROI) were applied to thermal photographs and average temperatures were calculated using Thermovison ExaminIR Beta software (FLIR Inc., Wilsonville, OR). The BAT ROI covered the shaved area from the back of the skull to the bottom of the shoulder blades, while the Body ROI spanned the remaining shaved area caudal the BAT ROI. Following temperature measurements, mice in groups A and B were adapted to oxymax chambers [Comprehensive Lab Animal Monitoring system (CLAMS); Columbus Instruments, Columbus, OH] and i.p. vehicle injections to minimize stress-induced energy expenditure. Then mice

received three days i.p. vehicle treatment (both groups, $n = 8$), followed by three days CNO treatment [i.p. 0.3 mg/kg body weight (group A, $n = 4$) or 1.5 mg/kg body weight (group B, $n = 4$)]. Animals were allowed to recover for one week after the last CNO injection. A number of mice from group A and C ($n = 11$) were adapted to the BioDAQ system (Research Diets Inc., New Brunswick, NJ) for a week and body weight and food intake was monitored daily during three days of vehicle injections and three days of CNO (0.3 mg/kg body weight) i.p. injections. Group A mice ($n = 4$) were again recovered for at least one week after the last CNO injection to test the effect of β_3-adrenergic antagonist SR 59230A (Sigma–Aldrich, St. Louis, MO) on CNO-induced energy expenditure. Animals were acclimated to new metabolic chambers (TSE Systems Inc., Chesterfield, MO) and received at least three days of i.p. vehicle, CNO (0.3 mg/kg body weight), and CNO + SR 59230A (0.3 mg/kg + 1 mg/kg body weight, respectively) injections over consecutive days during which energy expenditure was recorded continuously.

2.6. Measurement of body temperature, energy expenditure, activity, body weight/composition, and food intake in control and AAV-cre mice

Beginning at two weeks prior to AAV-cre injection, two cohorts of $LepRb^{fl/fl}$ mice (control virus, $n = 6$ and AAV-cre, $n = 5$) were monitored for daily body weight and food intake over eight weeks. One week prior to AAV-cre injection, mice were adapted to oxymax chambers to minimize stress-induced energy expenditure. Then mice were monitored for baseline energy expenditure and activity across two days. Immediately prior to AAV-cre injection, rectal temperature was recorded and body composition was determined by NMR (minispec-mq series; Bruker, Billerica, MA). Following AAV-cre injection, mice were continually monitored for body weight and food intake. Every other week rectal temperature was recorded, body composition was determined by NMR, and mice were returned to oxymax chambers for energy expenditure and activity recordings. After recovering from the last oxymax recordings, mice were placed in a 4 °C environmental chamber and rectal temperatures were monitored every 30 min for three hours. At the completion of all physiological recordings, mice were fasted for 24 h, injected with leptin (5 mg/kg, i.p.) and perfused after an hours of incubation to determine leptin-induced pSTAT3 by histochemical analysis as an indicator of functional LepRb expression.

2.7. Brain slices, whole-cell patch-clamp recordings and histology

Acute brain slices were prepared as previously described [26,27]. Briefly, under isofluorane anesthesia the brain was removed and immersed in ice-cold oxygenated artificial cerebrospinal fluid (aCSF) containing the following (in mM): 124 NaCl, 26 $NaHCO_3$, 1.4 NaH_2PO_4, 11 glucose, 3 KCl, 1.3 $MgCl_2$, 1.5 $CaCl_2$, pH 7.3–7.4. Coronal hypothalamic slices (300 μm) containing the DHA/DMH were made using a vibrating microtome (Vibratome Series 1000; Warner Instruments, Hamden, CT). The slices were stored in a holding chamber at 34–37 °C, and then transferred to a recording chamber mounted on a fixed stage under an upright microscope (Nikon FN1; Nikon Instrument Inc., Melville, NY).Whole-cell patch-clamp recordings were performed at 34–37 °C from DHA/DMH neurons expressing AAV-DREADD, which were identified by mCherry expression under a 40× water-immersion objective (N.A = 0.8). Epifluorescence was used to visualize mCherry-expressing neurons and infrared differential interference contrast optics (IR-DIC) to target specific cells. For whole-cell patch-clamp recordings, electrodes (3–7 MΩ) were filled with a solution containing with following (in mM): 130 K^+ gluconate, 10 HEPES, 5 EGTA, 1 NaCl, 1 $MgCl_2$, 1 $CaCl_2$, 3 KOH, 2–3 Mg-ATP, 0.2% biocytin, pH 7.3–7.4. Electrophysiological signals were recorded using an Axoclamp 700B amplifier (Molecular Devices, Sunnyvale, CA) and acquired by pClamp (Molecular Devices, Sunnyvale, CA). Action potentials were analyzed offline using pClamp and Mini-Analysis (Synaptosoft, Decatur, GA). CNO (5 μM; Sigma, St. Louis, MO) was dissolved in 0.05% DMSO in aCSF. After recordings brain slices were fixed with 4% paraformaldehyde in 0.15 M sodium phosphate buffer overnight at 4 °C. After several rinse in 0.01 M phosphate buffered saline (PBS), slices were immersed in AMCA Avidin D (1:200; Vector Labs, Burlingame, CA) in 0.01 M PBS containing 1% Triton X-100 for 72 h at 4 °C to visualize the recorded neurons. Slices were then washed with 0.01 M PBS and mounted onto charged slides (Fisher Scientific, Waltham, MA), air dried, covered in an anti-oxidant medium (Vectashield; Vector Labs, Burlingame, CA) and coverslipped.

2.8. Perfusion and immunohistochemistry

Perfusions and immunohistochemistry were performed as described earlier [25]. Briefly, mice were deeply anesthetized with isoflurane and transcardially perfused with ice cold physiological saline for 30 s and ice cold 10% neutral buffered formalin (Sigma–Aldrich, St. Louis, MO) for 5 min. Brains were removed and either post fixed in formalin and cryoprotected in 30% sucrose before cryosectioning into 4 representative series of 30 μm sections or snap frozen on dry ice until cryosectioning. Sections were stained immunohistochemically as described elsewhere [18,23] using rabbit anti-phospho(Tyr705)STAT3 (1:2000, #9131; Cell Signaling, Danvers, MA), rabbit anti-cFos (1:10,000,#PC38; Millipore, Billerica, MA), goat anti-dsRed (1:1000, for detection of mCherry; Santa Cruz Biotechnology Inc, Santa Cruz, CA) and chicken-anti-GFP (1:1000, #ab13970; Abcam, Cambridge, MA) as primary antibodies. Nuclear peptides (cFos or pSTAT3) were stained first and developed with the diaminobenzidine (DAB) method. Staining with additional primary antibodies was performed and detected with fluorescent labeled secondary antibodies, Alexa568 (dsRed) or Alexa488 (GFP) from Life Technologies (Carlsbad, CA).

2.9. Neuronal cell count estimates

Immunohistochemical staining for cFos and GFP ($LepRb^{GFP}$ mice) was visualized with a fluorescent microscope (Olympus BX51; Center Valley, PA) and images were taken with a digital camera (Olympus DP30BW; Center Valley, PA) using appropriate filters for fluorophores or bright-field illumination for DAB stain. Images for cFos/GFP were taken at identical sites, superimposed, and pseudocolored using Olympus Software and Adobe Photoshop (Adobe Systems, San Jose, CA). Brightness and contrast were modified for all images to enhance visibility of nuclear cFos staining for figure preparation and cell counts, however, care was taken that all images within an experiment were modified with identical settings. For each brain (vehicle group, $n = 4$; leptin group, $n = 3$–5) two sections containing the compact DMH (Bregma level −1.7 to −2 mm, coordinates based on Paxinos Mouse Brain atlas [24]) were analyzed. Cell counts were performed in the DMH/DHA based on the distribution of $LepRb^{GFP}$ cells [18]. The DMH/DHA was defined as the area above the compact DMH up to the mammillary thalamic tract (mt). The total number of $LepRb^{GFP}$ cells and the number of cFos + $LepRb^{GFP}$ co-labeled cells was counted and co-localization of cFos was expressed as % cFos co-localization per $LepRb^{GFP}$ cells. For leptin-induced pSTAT3 cell counts (control and AAV-cre mice) bright-field images were taken from the DMH and the ARC. For each brain (control, $n = 6$; AAV-cre, $n = 4$) cell counts were obtained in the ventral, compact and dorsal DMH, as well as DHA, and in the ARC of three anatomically comparable hypothalamic sections. The total number of $pSTAT3^+$ neurons was compared between control and AAV-cre mice.

2.10. Statistical analyses

We compared differences between vehicle and leptin treated, vehicle and CNO treated, or control and AAV-cre virus injected groups with repeated measures ANOVA followed by a Holm—Sidak test for pairwise comparisons or student's *t*-test as specified in the figure legends. In instances of non-parametric distribution, Friedman repeated measures ANOVA on ranks was used as specified in the figure legends. Alpha levels were set at 0.05 for all analysis. SigmaPlot 11 (Systat Software Inc., San Jose, CA) or SAS/STAT (SAS Institute Inc., Cary, NC) software packages were used for all analyses.

3. RESULTS

3.1. Peripheral leptin treatment activates DMH/DHA LepRb-expressing neurons

Cold and pyrogen-stimulated BAT thermogenesis both work through the indirect activation of DMH/DHA neurons [17,28,29], and we have previously shown that acute cold-exposure activates DMH/DHA LepRb neurons [18]. To test if thermogenic leptin action occurs through a similar mechanism, we examined neuronal activation in DMH/DHA LepRb neurons in LepRb^{GFP} reporter mice following i.p. injection of leptin or vehicle. Neuronal activation was evaluated by quantifying the induction of cFos (a surrogate for neuronal activation) in DMH/DHA LepRb^{GFP} neurons. Leptin increased cFos two-fold in DMH/DHA LepRb neurons compared to vehicle treated mice ($p < 0.01$, $n = 3$—4, Figure 1A—C), indicating that leptin activates DMH/DHA LepRb neurons similar to acute cold exposure [18]. This further supports the hypothesis that leptin directly acts on DMH/DHA LepRb neurons to elevate energy expenditure and contributes to weight loss.

3.2. Pharmacogenetic activation of DMH/DHA LepRb neurons

We next determined whether the activation of DMH/DHA LepRb neurons is sufficient to stimulate BAT thermogenesis and energy expenditure. DREADDs are mutated muscarinic receptors that completely lack responsiveness for their endogenous ligand and instead they potently respond to nanomolar doses of the designer drug CNO [30,31]. CNO stimulation is thought to close KCNQ potassium channels via the Gq coupled designer receptor hM3Dq, resulting in intracellular Ca^{2+} flux and neuronal depolarization [32]. We injected AAV-DREADD [31] into the DMH/DHA of LepRb^{cre} mice (AAV-DREADD mice) to obtain restricted DREADD expression in DMH/DHA LepRb neurons. Correct AAV-DREADD injection sites and anatomical expression were verified by immunohistochemical detection of mCherry ("HIT" mice, Figure 2A) and distinguished from inaccurate AAV-DREADD injection sites or poor expression, that we labeled as "MISSED" injections (Figure 2B). A schematic drawing of the rostro-caudal viral spread of "HIT" AAV-DREADD mice is also depicted across the three panels of Figure 3C. We confirmed the functionality of AAV-DREADD and show that CNO-induced cFos in mCherry^{+} neurons (Figure 2D—F), and that CNO bath application induced action potentials and depolarization in mCherry^{+} DMH/DHA LepRb neurons using patch-clamp electrophysiological recordings in brain slices (Figure 2G,H).

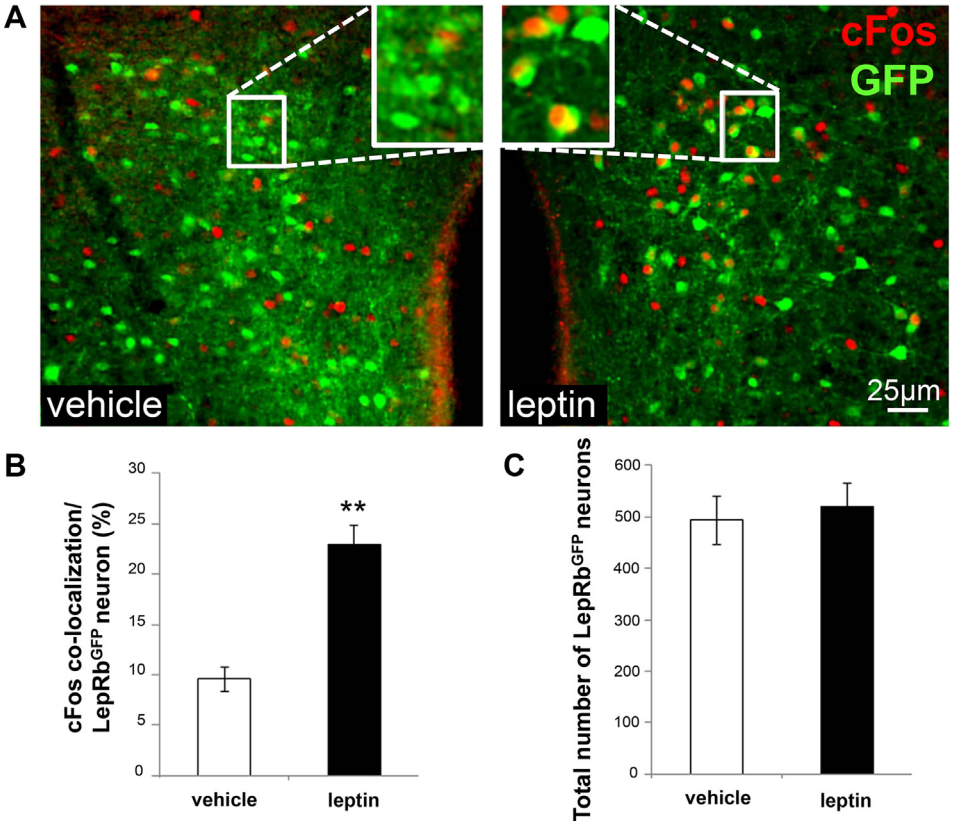

Figure 1: DMH/DHA LepRb neurons are activated by leptin. **A**. Representative images of LepRb^{GFP} reporter mice three hours after acute i.p. vehicle (left panel, $n = 3$) or leptin (5 mg/kg body weight, right panel, $n = 4$) treatment. Sections were stained for cFos as a surrogate for neuronal activation and GFP as a surrogate for LepRb neurons. **B**. Percentage of LepRb^{GFP} neurons that are co-localized with cFos within the DMH/DHA. $^{**}p^{t\text{-test}} < 0.01$. **C**. Total number of LepRb^{GFP} neurons in the DMH/DHA.

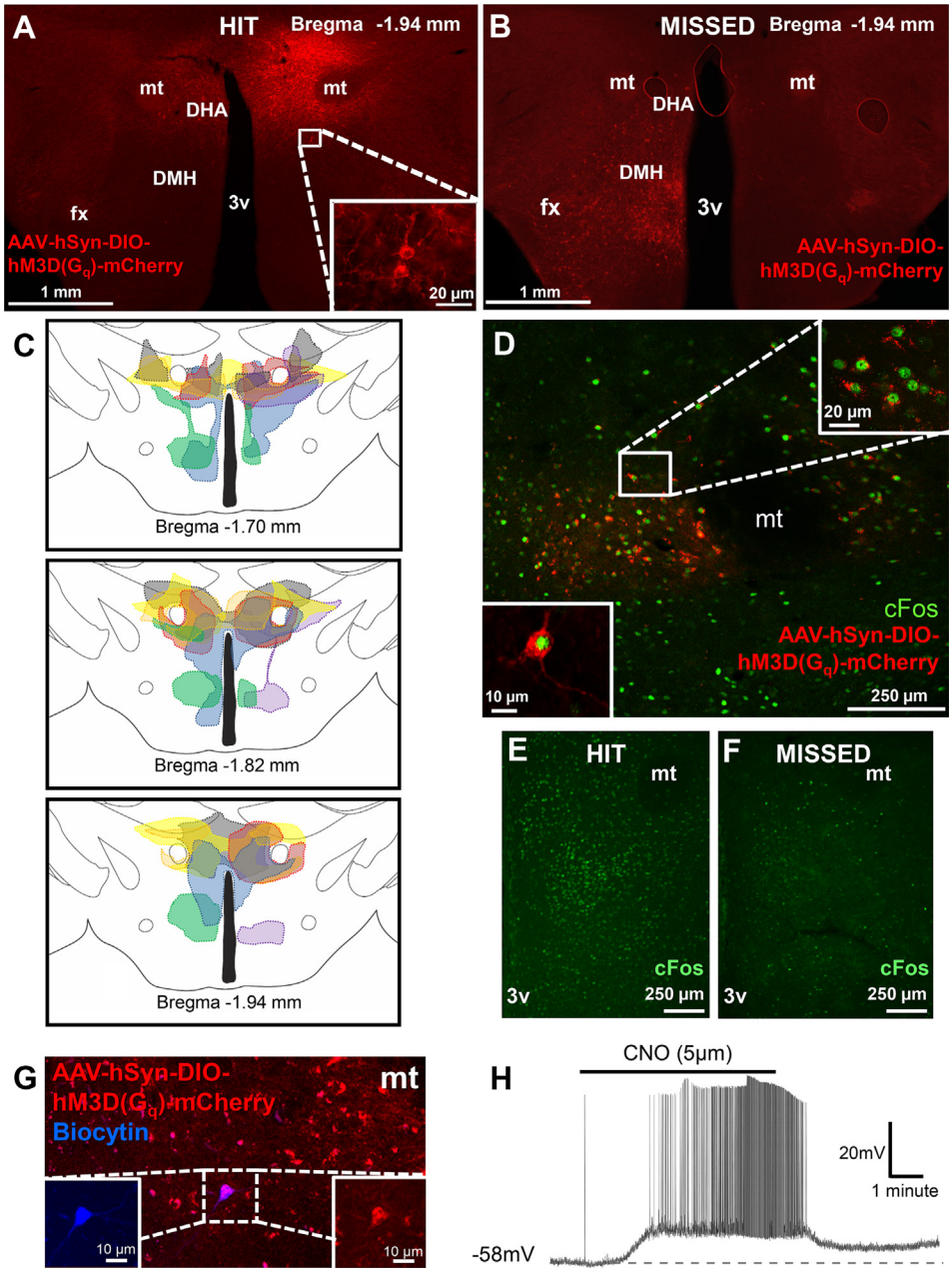

Figure 2: AAV-DREADD expression and functionality in DMH/DHA LepRb neurons. Representative images of AAV-DREADD expression in LepRb^{cre} mice injected with AAV-hSyn-DIO-hM3D(G_q)-mCherry showing a "HIT" (**A.**) or "MISSED" (**B.**) injection into the DMH/DHA. **C**. Schematic representation of viral/mCherry spread across the DMH/DHA. D. Two hours after an acute i.p. CNO injection (1.5 mg/kg), cFos is robustly induced in mCherry$^+$ neurons of "HIT" mice (**E.**), but not "MISSED" mice (**F.**). **G**. Representative image of a successfully patched mCherry$^+$ neuron labeled with biocytin. **H**. CNO bath application depolarized the recorded mCherry$^+$ neuron leading to burst firing of action potentials. 3v, third ventricle; DHA, dorsal hypothalamic area; DMH, dorsomedial hypothalamus; fx, fornix; mt, mammillothalamic tract.

3.3. Activation of DMH/DHA LepRb neurons increases BAT and body temperature

We further tested the thermogenic effect of DMH/DHA LepRb activation by measuring body temperature. First, we monitored skin temperature with an infrared/thermal camera, which does not require handling of the animals and thus prevents stress induced rises in body temperature. Furthermore, we could spatially distinguish skin temperature at the level of the intrascapular BAT and the lower body in AAV-DREADD mice after CNO (1.5 mg/kg BW, i.p.) or vehicle injection. Thermal imaging revealed significant increases in skin temperature with CNO treatment, when compared to vehicle ($p < 0.05$ and 0.01; Figure 3B and C, respectively). BAT and lower body temperature increased with similar magnitudes and chronology following CNO treatment, suggesting that BAT thermogenesis was neither the initial nor the sole source of thermogenesis. An immediate rise in body temperature after CNO treatment was also demonstrated with subcutaneously implanted transmitters ($p < 0.001$; Figure 3D) and by measurement of rectal temperature ($p < 0.001$; Figure 3E). In all cases body temperature did not increase more that 1–1.5 °C, well within normal physiological range and far from eliciting a fever response.

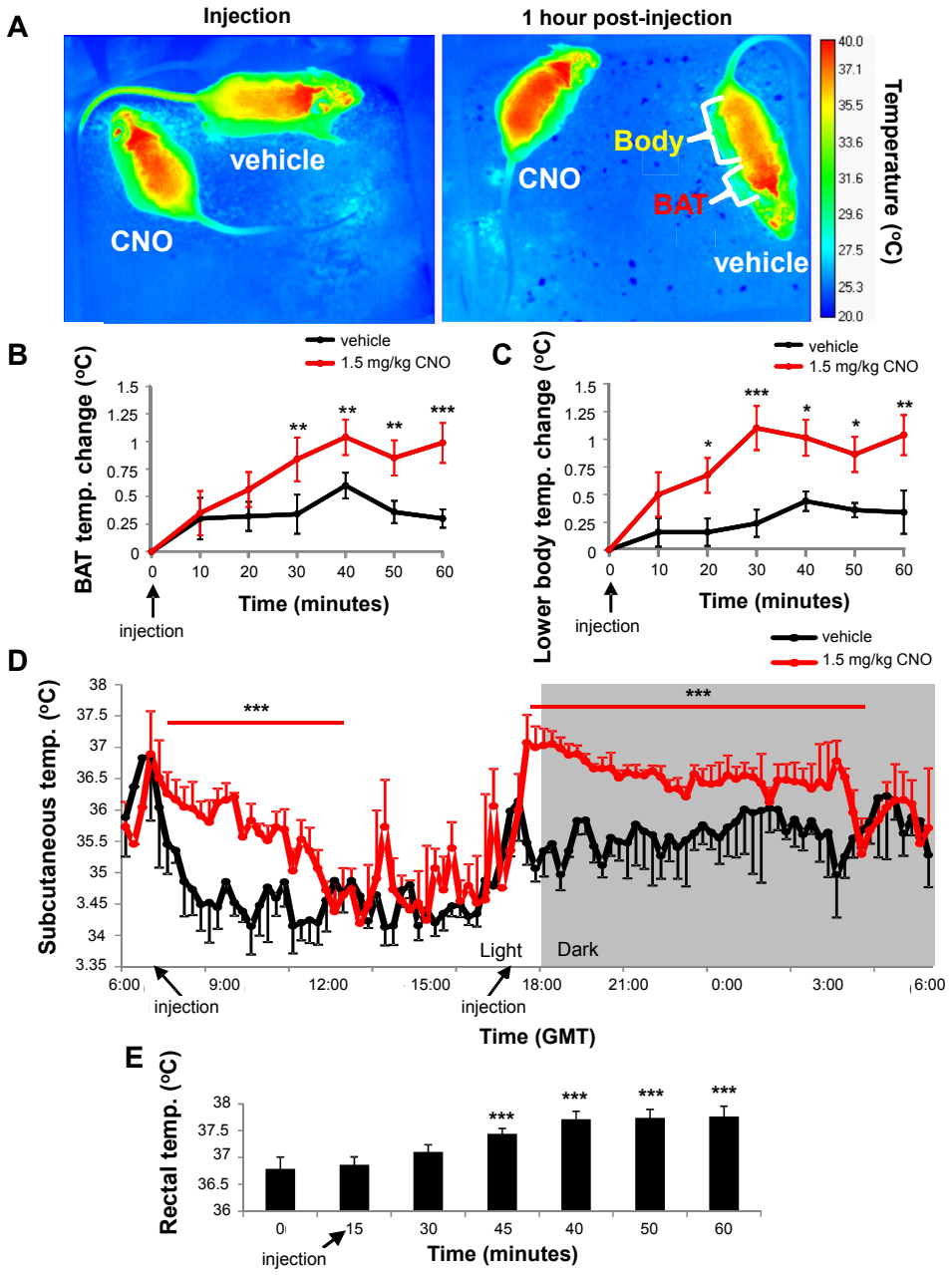

Figure 3: Activation of DMH/DHA LepRb neurons increases BAT and body temperature. **A**. Representative temperature images of AAV-DREADD mice after vehicle or CNO injections; immediately after injection (left panel) and 1 h post-injection (right panel). Images were taken every 10 min over 1 h to monitor temperature changes in the brown adipose tissue (BAT, intrascapular level, **B**. $p^{ANOVA} < 0.05$, $^{**}p^{post\text{-}hoc} < 0.01$, $^{***}p^{post\text{-}hoc} < 0.001$) and the lower body (**C**. $p^{ANOVA} < 0.01$, $^{*}p^{post\text{-}hoc} < 0.02$, $^{**}p^{post\text{-}hoc} < 0.01$, $^{***}p^{post\text{-}hoc} < 0.001$). **D**. Continuous subcutaneous temperature measurement using implanted minimitters in mice with DREADD expression in DMH/DHA LepRb neurons after a 1.5 mg/kg CNO injection ($n = 2$). $^{***}p^{ANOVA} < 0.001$. **E**. Rectal temperature of mice with AAV-DREADD expression in DMH/DHA LepRb neurons after a 0.3 mg/kg CNO injection ($n = 8$). $p^{ANOVA} < 0.001$, $^{***}p^{post\text{-}hoc} < 0.001$. GMT, Greenwich Mean Time.

3.4. Activation of DMH/DHA LepRb neurons induces energy expenditure, locomotor activity, and body weight loss

We next evaluated the impact of DMH/DHA LepRb neuronal activation on energy expenditure with indirect calorimetry. CNO injections (i.p. 0.3 or 1.5 mg/kg body weight) raised energy expenditure robustly and dose-dependently within minutes ($p < 0.001$), peaking after an hour and returning to normal within four to five hours (Figure 4A). Increased energy expenditure was further accompanied by an increase in total locomotor activity ($p < 0.02$ and $p < 0.001$, respectively; Figure 4B), further suggesting that the profound induction of energy expenditure does not arise exclusively from BAT thermogenesis but also from increased locomotor activity. Following three days of consecutive CNO treatment, correctly targeted "HIT" mice showed a significant reduction in body weight compared to vehicle treatment ($p < 0.001$, Figure 4C). CNO dependent changes in energy expenditure and body weight were only observed in "HIT" mice. Mice with "MISSED" injections, showed no changes in energy expenditure or body weight with CNO treatment (Figure 4D and E, respectively). DREADD mediated activation of DMH/DHA LepRb neurons did not affect food intake (Figure 4F), demonstrating that

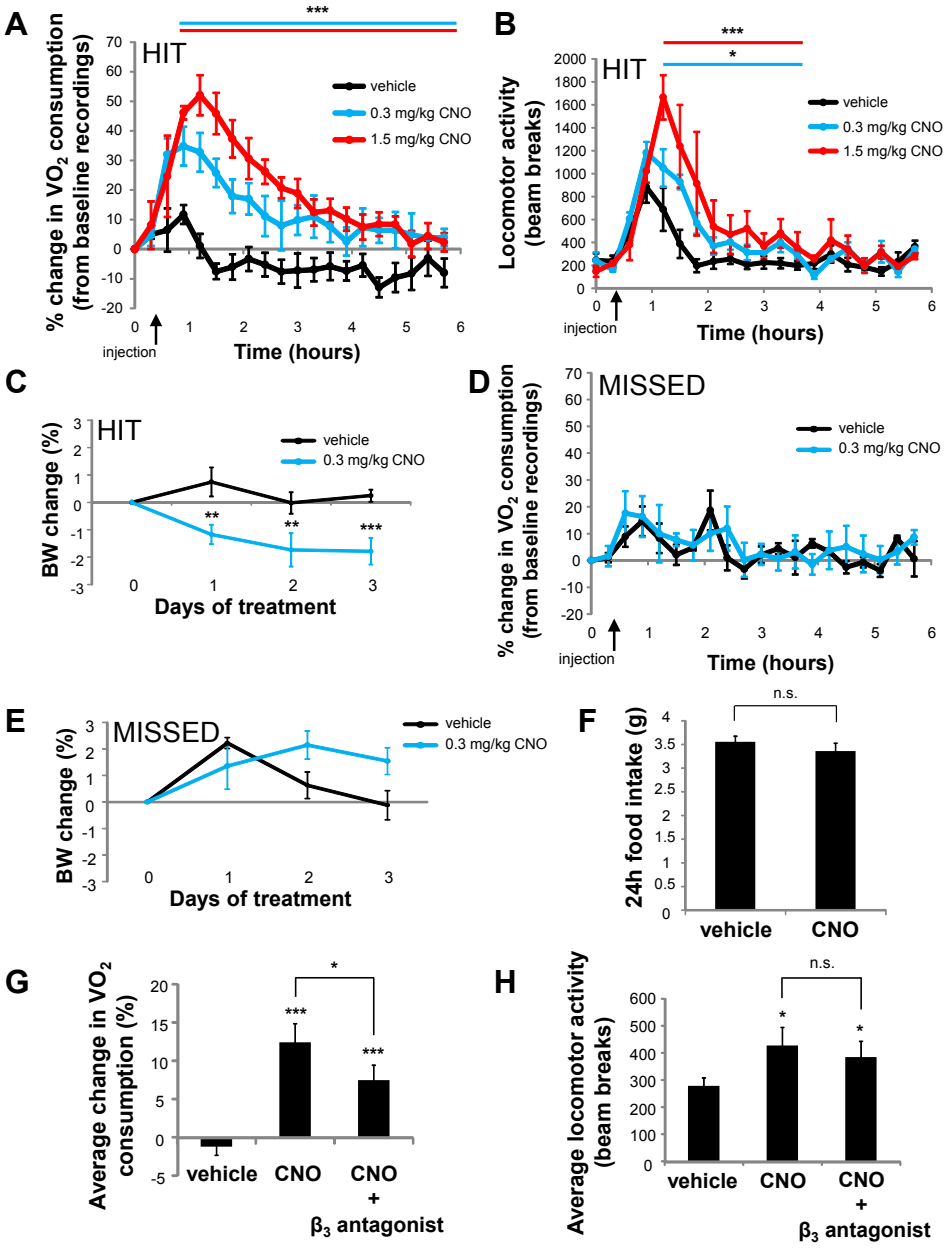

Figure 4: Activation of DMH/DHA LepRb neurons induces energy expenditure, locomotor activity, and body weight loss. **A**. **"HIT" mice,** percent change in oxygen consumption [after i.p. saline ($n = 8$) or CNO (0.3 and 1.5 mg/kg body weight, $n = 4$ per dose) injections]. $^{***}p^{ANOVA} < 0.001$. **B**. **"HIT" mice,** locomotor activity [after i.p. saline ($n = 8$) or CNO (0.3 and 1.5 mg/kg body weight, $n = 4$ per dose) injections]. $^{*}p^{ANOVA} < 0.02$, $^{***}p^{ANOVA} < 0.001$. **C**. **"HIT" mice,** body weight change during 3 days of vehicle or CNO (0.3 mg/kg body weight) treatment ($n = 8$). $p^{ANOVA} < 0.001$; $^{*}p^{post\text{-}hoc} < 0.05$, $^{**}p^{post\text{-}hoc} < 0.01$. **D**. **"MISSED" mice,** percent change in oxygen consumption [after i.p. saline ($n = 3$) or CNO (0.3 and 1.5 mg/kg body weight, $n = 4$ per dose) injections]. **E**. **"MISSED" mice,** body weight change during three days of vehicle or CNO (0.3 mg/kg body weight) treatment ($n = 3$). In cases with insufficient AAV-DREADD expression or poor DMH/DHA targeting, CNO was unable to increase energy expenditure or decrease body weight (**D**. and **E**.). **F**. **"HIT" mice,** 24 h food intake after three days of i.p. vehicle or CNO treatment [0.3 mg/kg body weight ($n = 4$)]. **G**. **"HIT" mice,** average change in oxygen consumption (three hours post-injections) after vehicle, CNO (0.3 mg/kg body weight) and CNO + β_3-antagonist (SR 59230A, 1 mg/kg body weight), $n = 4$ per group, $p^{ANOVA} < 0.001$; $^{*}p^{post\text{-}hoc} < 0.02$, $^{***}p^{post\text{-}hoc} < 0.001$ (vs. vehicle). **H**. **"HIT" mice,** average locomotor activity (three hours post-injections) after vehicle, CNO (0.3 mg/kg body weight) and CNO + β_3-antagonist (SR 59230A, 1 mg/kg body weight). $n = 4$ per group, $p^{ANOVA} < 0.03$; $^{*}p^{post\text{-}hoc} < 0.05$.

changes in body weight were solely attributable to changes in energy expenditure.

Sympathetic induction of BAT thermogenesis is initiated via β_3-adrenergic receptor signaling in BAT adipocytes. To determine the extent to which classic BAT thermogenesis contributes to CNO-induced energy expenditure (compared to total locomotor activity), we tested whether β_3-adrenergic receptor blockade would abolish this effect. β_3-adrenergic blockade attenuated CNO-induced energy expenditure significantly, but incompletely ($p < 0.05$; Figure 4G); further supporting that CNO-induced energy expenditure is not exclusively mediated by β_3-dependent BAT thermogenesis. Indeed, β_3-adrenergic blockade did not affect CNO-induced locomotor activity (Figure 4H), indicating that CNO-induced energy expenditure results from β_3-dependent induction of BAT thermogenesis and β_3-independent induction of locomotion.

3.5. Intra-DMH/DHA leptin administration corrects hypothermia in *ob/ob* mice

To test the physiological relevance of DMH/DHA LepRb neurons in leptin-stimulated thermogenesis, we injected leptin or vehicle into the DMH/DHA of leptin-deficient *ob/ob* mice and control littermates twice daily over three days. Correct cannula placement was verified anatomically after the experiment (Figure 5B). As expected, all *ob/ob* mice were hypothermic and obese before leptin treatment compared to their control littermates ($p < 0.0002$, data not shown). Leptin treatment had no measureable effect on body temperature in wildtype littermates at the end of the three day treatment, while intra-DMH/DHA leptin injection in *ob/ob* mice normalized hypothermia to body temperatures comparable to control littermates (Figure 5C). Leptin also significantly elevated body temperature in *ob/ob* mice compared to vehicle treated *ob/ob* mice ($p < 0.02$; Figure 5C). Leptin treatment also trended towards suppressing body weight gain in *ob/ob* mice compared to vehicle treated *ob/ob* mice, even though data did not reach statistical significance ($p < 0.07$; Figure 5D). In line with our previous observations in Figure 4F, activation of LepRb neurons via intra-DMH/DHA leptin administration did not affect food intake (Figure 5E).

3.6. Blockade of DMH/DHA leptin signaling impairs acute thermoregulatory responses, increases body weight, and augments food intake

To validate that leptin action on DMH/DHA LepRb neurons *per se* is physiologically relevant for energy homeostasis, we selectively depleted LepRb from DMH/DHA neurons by injecting AAV-cre or control virus into $LepRb^{fl/fl}$ mice (AAV-cre and control mice, respectively). Spatially confined, accurate AAV-cre injection sites and anatomical AAV-cre expression were verified by IHC detection of GFP ("HIT" mice, Figure 6A). Brains from mice with inaccurate injection sites or poor viral expression were excluded from analysis. Adequate ablation of LepRb in DMH/DHA neurons was further confirmed by quantification of leptin-induced pSTAT3 in the hypothalamus of AAV-cre and control mice. AAV-cre mice showed significant less leptin-induced pSTAT3 specifically in the DMH/DHA compared to control mice, while other hypothalamic sites, like the ARC, remained fully responsive to leptin (Figure 6B–D). Leptin-induced pSTAT3 was reduced by 50% in the DMH (including the ventral, compact and dorsal portion of the DMH, and DHA) of AAV-cre mice compared to controls, while the ARC remained fully responsive to leptin ($p < 0.05$; Figure 6D). At room temperature AAV-cre mice exhibited no differences in rectal temperatures when compared to controls, but acute 4 °C cold exposure revealed that AAV-cre mice defended their body temperature less efficiently over the first two hours of cold exposure ($p < 0.01$; Figure 6E), even though rectal temperature was equally low in both groups after three hours in the cold.

Furthermore, AAV-cre mice showed a robust time-dependent weight gain immediately following virus-injection ($p < 0.001$; Figure 6F). NMR analysis showed that this was mostly due to a significant time-dependent accumulation of fat mass ($p < 0.001$; Figure 6G), although an increase in lean mass was also apparent five weeks following AAV-cre injection ($p < 0.05$; Figure 6G). Food intake relative to lean body mass also rose substantially in AAV-cre mice during the first two weeks following viral injections, but tapered off after that and became indistinguishable from control mice after three weeks post-

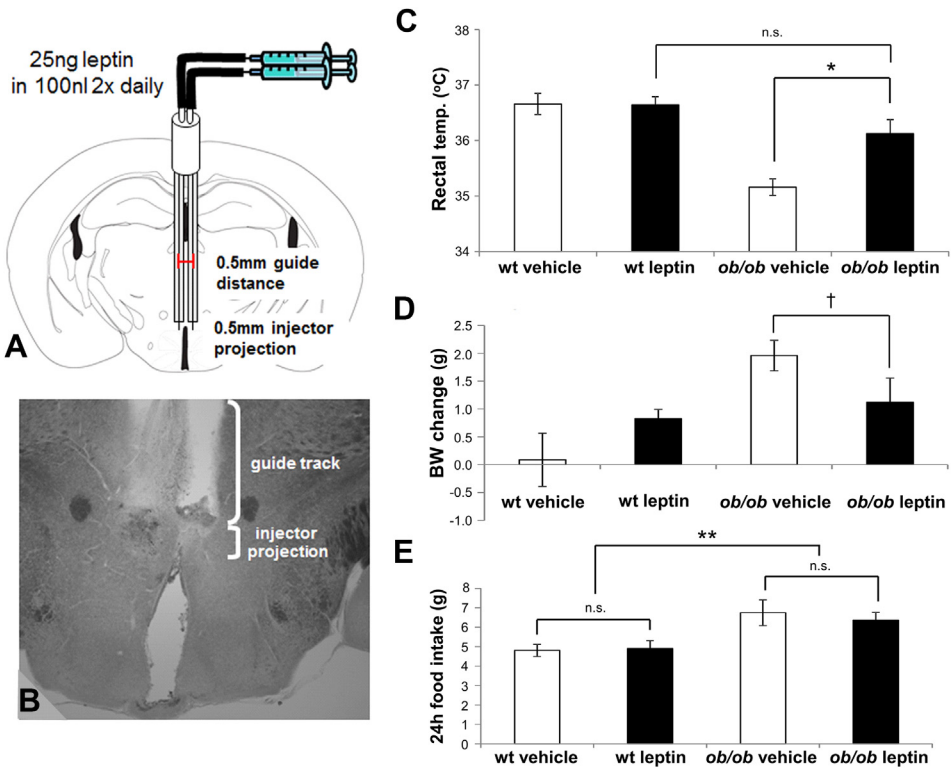

Figure 5: Intra-DMH/DHA leptin injections correct hypothermia in leptin-deficient *ob/ob* mice. **A**. Schematic drawing of bilateral cannulations of the DMH/DHA area. **B**. Example of the anatomical verification of correctly cannulated DMH/DHA. **C**. Rectal body temperature of vehicle treated wildtype mice ($n = 8$), vehicle treated *ob/ob* mice ($n = 5$), leptin treated wildtype mice ($n = 8$), and leptin treated *ob/ob* mice ($n = 6$) after three consecutive days of treatment. $^{*}p^{\text{post-hoc}} < 0.02$. **D**. Body weight change after three consecutive days of vehicle or leptin treatment. $^{\dagger}p^{\text{t-test}} < 0.07$. **E**. 24 h food intake during three days of vehicle injections and during three days of leptin injections. wt, wildtype.

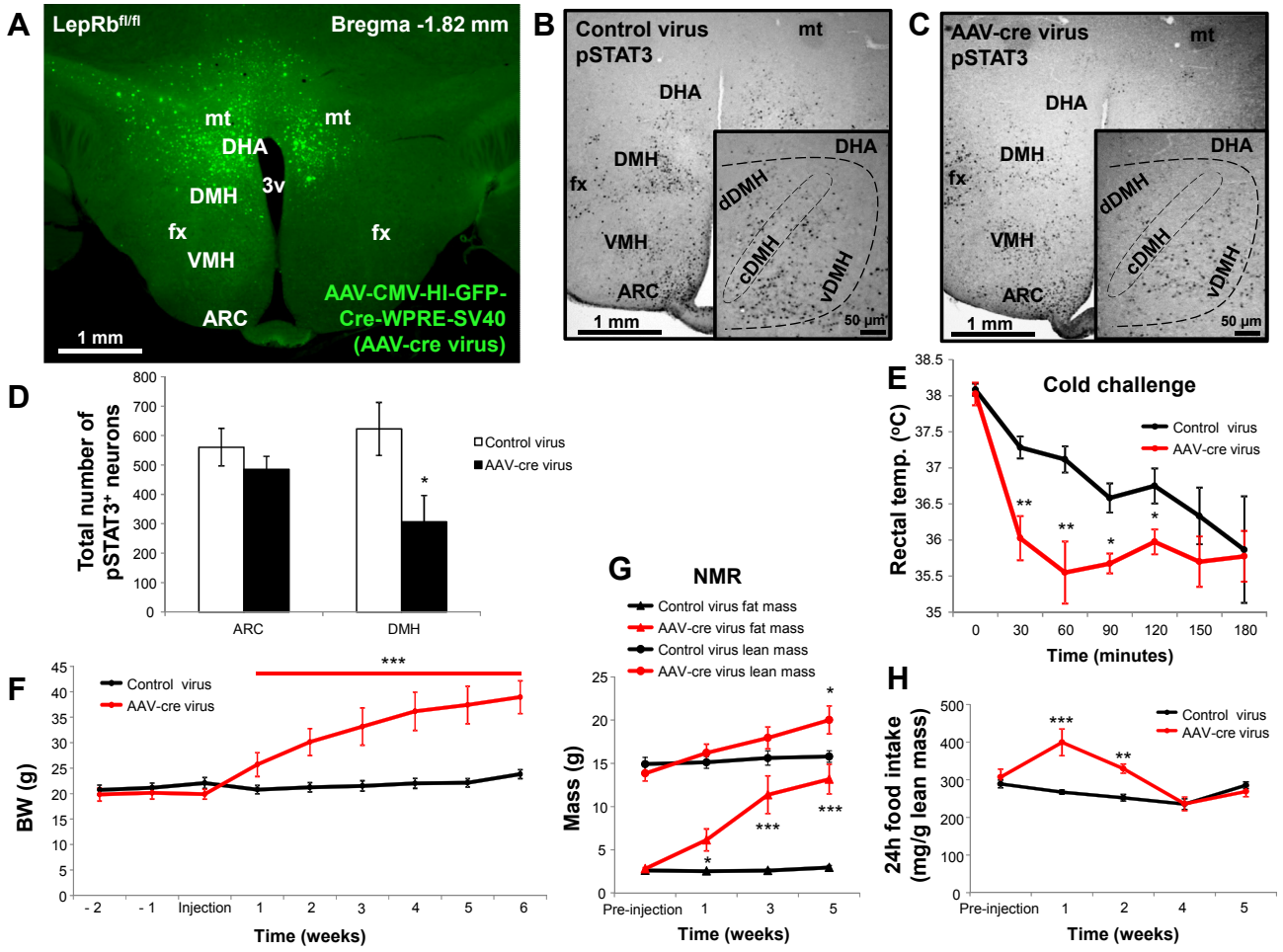

Figure 6: Blockade of DMH/DHA leptin signaling impairs acute thermoregulatory responses, increases body weight, and augments food intake. **A**. Representative image of AAV-cre expression/LepRb deletion in the DMH/DHA of a properly targeted mouse. Representative images of hypothalamic pSTAT3 induction following leptin treatment (i.p., 5 mg/kg for an hour) of control (**B**.) or AAV-cre virus mice (**C**.). Sections were stained for pSTAT3 as a surrogate for functional LepRb signaling. **D**. Cell counts of pSTAT3^{+} neurons in the ARC and DMH/DHA of control and AAV-cre injected mice. $*p^{\text{t-test}} < 0.05$. **E**. Rectal temperature of control ($n = 6$) and AAV-cre ($n = 5$) injected mice during a 4 °C cold challenge over three hours. $p^{\text{ANOVA}} < 0.001$; $*p^{\text{post-hoc}} < 0.02$, $**p^{\text{post-hoc}} < 0.01$. **F**. Weekly body weight of control and AAV-cre mice over eight weeks. $***p^{\text{ANOVA}} < 0.001$. **G**. Body composition of control and AAV-cre mice over eight weeks. Fat mass: $p^{\text{ANOVA}} < 0.001$; $*p^{\text{post-hoc}} < 0.02$, $***p^{\text{post-hoc}} < 0.001$; lean mass: $*p^{\text{t-test}} < 0.05$. **H**. Daily food intake per lean body mass of control and AAV-cre mice over eight weeks. $**p^{\text{t-test}} < 0.01$, $***p^{\text{t-test}} < 0.001$. 3v, third ventricle; ARC, arcuate nucleus; cDMH, compact part of the dorsomedial hypothalamus; DHA, dorsal hypothalamic area; dDMH, dorsal part of the dorsomedial hypothalamus; DMH, dorsomedial hypothalamus; fx, fornix; mt, mammillothalamic tract; VMH, ventromedial hypothalamus.

injection (Figure 6H). Therefore, the ongoing rise in body weight at weeks post-injection and beyond is largely food intake-independent.

3.7. Blockade of DMH/DHA leptin signaling reduces energy expenditure and locomotor activity

The transiently increased food intake does not entirely explain the magnitude and ongoing body weight change observed in AAV-cre mice. Thus, we further examined if changes in energy expenditure accounted for the changes in body weight. We performed indirect calorimetry in mice at six weeks post-injection and found a significant decrease in energy expenditure that was most robust during the dark phase of the day ($p < 0.001$; Figure 7A,B). In addition, there was a marked reduction in the total locomotor activity of AAV-cre mice, specifically, during the dark phase ($p < 0.001$; Figure 7C,D). Taken together, the above data show that the phenotype observed after LepRb deletion from DMH/DHA neurons is the exact opposite of that observed following pharmacogenetic activation of DMH/DHA LepRb neurons. Thus direct leptin action on DMH/DHA LepRb neurons is a key mechanism to maintain proper energy expenditure and body weight control.

4. DISCUSSION

Leptin plays an important role in body weight maintenance through regulation of food intake and energy expenditure. Several distinct populations of LepRb-expressing neurons have been recently highlighted that mediate distinct aspects of anorexic leptin action [33–37], even though many other LepRb-expressing populations remain uncharacterized. Our study investigated the physiological importance of DMH/DHA LepRb neurons to regulate energy metabolism and body weight, which was based on our earlier work suggesting that DMH/DHA LepRb neurons contribute to BAT-related thermoregulatory circuits [18]. We show that neuronal activation of DMH/DHA LepRb neurons is sufficient to induce a robust increase in energy expenditure and a significant decrease in body weight. We also demonstrate that LepRb expression on DMH/DHA neurons is necessary for

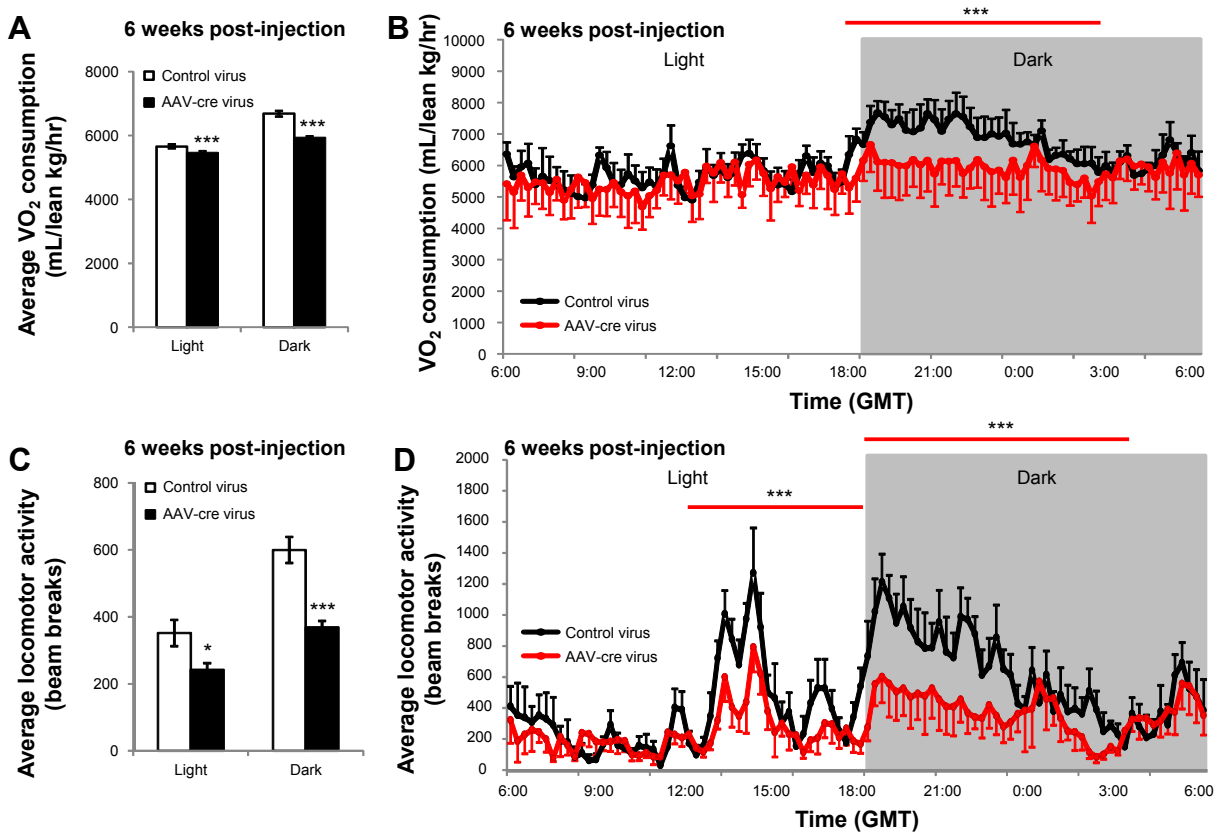

Figure 7: Blockade of DMH/DHA leptin signaling reduces energy expenditure and locomotor activity. **A**. Average oxygen consumption (per lean body mass) of control ($n = 6$) and AAV-cre ($n = 5$) mice at six weeks post-injection. $^{***}p^{\text{t-test}} < 0.001$. **B**. Average daily oxygen consumption (by lean body mass) of control and AAV-cre mice at six weeks post-injection. $^{***}p^{\text{ANOVA}} < 0.0001$. **C**. Average locomotor activity of control and AAV-cre mice at six weeks post-injection. $^{*}p^{\text{t-test}} < 0.05$, $^{***}p^{\text{t-test}} < 0.001$. **D**. Average daily locomotor activity of control and AAV-cre mice at six weeks post-injection. $^{***}p^{\text{ANOVA}} < 0.0001$. GMT, Greenwich Mean Time.

maintaining normal body weight, energy expenditure and body temperature. These findings indicate that baseline leptin action via DMH/DHA LepRb neurons opposes body weight gain by preventing hypometabolism.

DMH/DHA LepRb-mediated changes in energy expenditure and body weight are largely independent of food intake. Although blockade of leptin signaling evoked a transient surge in food intake, chow consumption relative to lean body mass returned to normal after three weeks of LepRb ablation. We speculate that the transient increase in food intake may compensate for impaired BAT thermogenesis and locomotion in order to maintain core body temperature [38–41], because rectal temperature remained normal unless animals were challenged with acute cold exposure. Taken together, our data highlight DMH/DHA LepRb neurons as the key mediator of thermoregulatory leptin action and a possible new drug target to selectively control energy expenditure and reduce body weight.

In accordance with our findings here, Enriori and colleagues [19] recently reported that intra-DMH leptin injections increased sympathetic BAT tone and body temperature. However, in contrast to our study, they showed that intra-DMH leptin administration acutely decreased food intake, while locomotor activity and body weight were not measured. We speculate that differences in the injection sites may explain these differences in food intake. In their study the entire DMH was targeted, while we specifically target the dorsal portion of the DMH and exclude the ventral portion of the DMH. Also, they use a four-fold higher leptin dose in a larger injection volume, so that leakage into more ventral LepRb neurons cannot be entirely ruled out. It is ultimately impossible to precisely track intra-parenchymal leptin diffusion.

We addressed these difficulties and stereotaxically targeted the DMH/DHA with viral constructs that allowed the visible confirmation and functional restriction of viral expression products to DMH/DHA LepRb neurons. Since low-dose CNO is physiologically inert and highly specific for DREADDs, we can conclude that the observed effects in AAV-DREADD mice are directly attributable to activated DMH/DHA LepRb neurons and reveals their remarkable capacity to evoke energy expenditure. Our data also indicate that leptin stimulates DMH/DHA LepRb neurons, even though leptin alone is unable to induce the same robust energy expenditure response [42,43]. A more pronounced leptin effect on energy expenditure is observed in leptin-deficient *ob/ob* mice [42,43], during fasting or food restriction where circulating leptin levels are low [10,11,44], or following ablation of LepRb from DMH/DHA neurons as demonstrated in this study. Since neuronal activation of DMH/DHA LepRb neurons is sufficient to potently increase energy expenditure, we speculate that leptin opposes afferent inhibitory signals that promote hypometabolism, but by itself is unable to fully override such inhibitory inputs. The chemical nature and anatomical sites of such inhibitory inputs remains to be identified in future studies.

Chao and colleagues recently found that loss of neuropeptide Y (NPY) expression in DMH neurons robustly increases energy expenditure [45]. Even though rat DMH NPY neurons do not co-express LepRb and changes in NPY gene expression are leptin-independent [46], mouse DMH NPY neurons are sensitive to leptin and show the presence of

leptin signaling [47]. Thus, the exact central circuits modulated by DMH NPY neurons are unclear. DMH NPY neurons regulate sympathetic outflow to the BAT and likely interact with presympathetic motor neurons, which may involve direct innervation of RPa neurons, or indirect circuits via the DMH/DHA.

Within the DMH and adjacent lateral hypothalamus orexin-expressing neurons innervate the RPa and orexin stimulates BAT thermogenesis via this circuit [48,49]. It is unknown whether DMH/DHA LepRb neurons may also innervate orexin neurons to regulate BAT thermogenesis and locomotor activity. However, since leptin primarily inhibits orexin neurons [50], it is unlikely that thermoregulatory leptin action is carried out via orexin neurons.

Melanocortins from the ARC act via melanocortin-4-receptors (MC4R) and regulate energy expenditure at the level of hindbrain preganglionic sympathetic neurons [51], as well as the DMH as suggested by Enriori and colleagues [19]. In addition, Kong and colleagues [52] recently described another thermogenic ARC based circuit, involving the paraventricular nucleus (PVN) and nucleus of the solitary tract, that feeds into the RPa. The brainstem also mediates thermogenic leptin action independent of hypothalamic inputs and elicits potent synergistic effects with other thermogenic hormones like thyroid stimulating hormone [53,54]. These brainstem circuits likely involve LepRb inputs to the RPa [55]. Thus, the RPa is well positioned to integrate inputs from several hypothalamic and extra-hypothalamic sites into an appropriate thermogenic response [56]. DMH/DHA LepRb neurons project directly to the RPa as well as the PVN [18] and the relative importance of such DMH/DHA LepRb projections in the regulation of energy expenditure will require further studies.

Surprisingly, we found that activation of DMH/DHA LepRb neurons also induced locomotor activity, while lack of stimulatory leptin signaling decreased locomotor activity. Locomotor activity includes measures of fine movements such as shivering and grooming [57,58], which may have contributed to the observed changes in locomotor activity. The neuronal activation level of DMH neurons is associated with shivering and locomotor activity [59,60]. Ablation of LepRb from DMH/DHA neurons removes stimulatory leptin inputs and the observed reduction in locomotor activity and reduced cold-resistance are in line with compromised shivering after inhibition of DMH neurons [59]. Activation of DMH/DHA LepRb neurons conversely increases locomotor activity in our studies, similar to increased locomotor activity after disinhibition of DMH neurons [60].

About 50% of DREADD-induced energy expenditure can be attributed to β_3-dependent mechanisms, indicating that BAT thermogenesis contributes to only half of the observed energy expenditure response. Locomotor activity was unaffected by β_3-adrenergic blockade and thus likely accounts for the remaining half of the energy expenditure response. DMH/DHA neurons are not retrogradely labeled from muscle, but instead PVN and rRPa neurons are strongly labeled with pseudorabies virus following intramuscular injection [61]. However, DMH LepRb neurons innervate the rRPa as well as the PVN [18] and it is likely that dorsal DMH/DHA LepRb neurons provide input to both the PVN and rRPa. Interestingly, while β_3-adrenergic receptors are the most commonly associated with BAT thermogenesis, only disruption of all three β-adrenergic receptor subtypes (but not single receptor deletions) caused increased sensitivity to high fat diet induced obesity [62]. While β_3-adrenergic receptors are only expressed in BAT, β_1- and β_2-adrenergic receptors are expressed in BAT and skeletal muscle. This expression pattern suggests that a complete thermogenic response, whether elicted by cold-, inflammation- or diet, not only involves several β-adrenergic receptors, but also engages at least two peripheral tissues, BAT and skeletal muscle. Our data indicate that DMH/DHA LepRb neurons induce energy expenditure via BAT-thermogenesis and locomotor activity with similar magnitudes and chronology, suggesting that both thermogenic mechanisms are initiated by the activation DMH/DHA LepRb neurons.

To date, leptin has been disappointing as a treatment for common human obesity, mostly due to hyperleptinemia and the consequent leptin resistance [9] that is associated with increased adiposity. Leptin levels drop quickly with fasting or food restriction and cause a state of low energy expenditure, which strongly counteracts weight loss in humans. When leptin levels return to pre-dieting/pre-weight loss levels, energy expenditure rises in turn, and body weight maintenance is restored in spite of increased food intake [10,11,63]. This phenomenon suggest that, while the anorexigenic effects of leptin may be self-limited, the thermoregulatory actions of leptin may prevent the counter-regulatory hypometabolic state associated with dieting. Therefore, an understanding of these central thermoregulatory circuits is critical to develop pharmacologic interventions to enhance or maintain body weight loss by preventing diet-induced hypometabolism in humans.

ACKNOWLEDGMENTS

This work was supported by P/F DK020572-30, NIH P20-RR02195, P/F NORC #2P30-DK072476-06, R01-DK092587 (HM), DK099598 (AZ), P30-GM103337 (AVD), and F32-DK097896 (KRZ). This work utilized the facilities of the Cell Biology and Bioimaging Core and Phenotyping Core, supported in part by COBRE (NIH P20-RR021945), CNRU (NIH 1P30-DK072476) center grants from the National Institutes of Health.

CONFLICT OF INTEREST

The authors declare no conflict of interest.

REFERENCES

[1] Haynes, W.G., Morgan, D.A., Walsh, S.A., Mark, A.L., Sivitz, W.I., 1997. Receptor-mediated regional sympathetic nerve activation by leptin. Journal of Clinical Investigation 100:270—278.

[2] Richards, R.J., Blalock, A., Liao, J., Reisin, E., 2003. Leptin: sympathetic and cardiovascular effects. Current Cardiology Reports 5:453—458.

[3] Gavrilova, O., Leon, L.R., Marcus-Samuels, B., Mason, M.M., Castle, A.L., Refetoff, S., et al., 1999. Torpor in mice is induced by both leptin-dependent and -independent mechanisms. Proceedings of the National Academy of Sciences of the United States of America 96:14623—14628.

[4] Davis, T.R., Mayer, J., 1954. Imperfect homeothermia in the hereditary obese-hyperglycemic syndrome of mice. American Journal of Physiology 177:222—226.

[5] Joosten, H.F., van der Kroon, P.H., 1974. Role of the thyroid in the development of the obese-hyperglycemic syndrome in mice (ob ob). Metabolism 23:425—436.

[6] Himms-Hagen, J., 1985. Defective brown adipose tissue thermogenesis in obese mice. International Journal of Obesity 9(Suppl. 2):17—24.

[7] Commins, S.P., Watson, P.M., Frampton, I.C., Gettys, T.W., 2001. Leptin selectively reduces white adipose tissue in mice via a UCP1-dependent mechanism in brown adipose tissue. American Journal of Physiology. Endocrinology and Metabolism 280:E372—E377.

[8] Heymsfield, S.B., Greenberg, A.S., Fujioka, K., Dixon, R.M., Kushner, R., Hunt, T., et al., 1999. Recombinant leptin for weight loss in obese and lean adults: a randomized, controlled, dose-escalation trial. Journal of the American Medical Association 282:1568—1575.

[9] Frederich, R.C., Hamann, A., Anderson, S., Lollmann, B., Lowell, B.B., Flier, J.S., 1995. Leptin levels reflect body lipid content in mice: evidence for diet-induced resistance to leptin action. Nature Medicine 1:1311–1314.
[10] Rosenbaum, M., Goldsmith, R., Bloomfield, D., Magnano, A., Weimer, L., Heymsfield, S., et al., 2005. Low-dose leptin reverses skeletal muscle, autonomic, and neuroendocrine adaptations to maintenance of reduced weight. Journal of Clinical Investigation 115:3579–3586.
[11] Galgani, J.E., Greenway, F.L., Caglayan, S., Wong, M.L., Licinio, J., Ravussin, E., 2010. Leptin replacement prevents weight loss-induced metabolic adaptation in congenital leptin-deficient patients. Journal of Clinical Endocrinology and Metabolism 95:851–855.
[12] Gilsanz, V., Chung, S.A., Jackson, H., Dorey, F.J., Hu, H.H., 2011. Functional brown adipose tissue is related to muscle volume in children and adolescents. Journal of Pediatrics 158:722–726.
[13] Wang, Q., Zhang, M., Ning, G., Gu, W., Su, T., Xu, M., et al., 2011. Brown adipose tissue in humans is activated by elevated plasma catecholamines levels and is inversely related to central obesity. PLoS ONE 6:e21006.
[14] Morrison, S.F., Nakamura, K., Madden, C.J., 2008. Central control of thermogenesis in mammals. Experimental Physiology 93:773–797.
[15] Nagashima, K., Nakai, S., Tanaka, M., Kanosue, K., 2000. Neuronal circuitries involved in thermoregulation. Autonomic Neuroscience 85:18–25.
[16] Dimicco, J.A., Zaretsky, D.V., 2007. The dorsomedial hypothalamus: a new player in thermoregulation. American Journal of Physiology – Regulatory, Integrative and Comparative Physiology 292:R47–R63.
[17] Yoshida, K., Li, X., Cano, G., Lazarus, M., Saper, C.B., 2009. Parallel preoptic pathways for thermoregulation. Journal of Neuroscience 29:11954–11964.
[18] Zhang, Y., Kerman, I.A., Laque, A., Nguyen, P., Faouzi, M., Louis, G.W., et al., 2011. Leptin-receptor-expressing neurons in the dorsomedial hypothalamus and median preoptic area regulate sympathetic brown adipose tissue circuits. Journal of Neuroscience 31:1873–1884.
[19] Enriori, P.J., Sinnayah, P., Simonds, S.E., Garcia Rudaz, C., Cowley, M.A., 2011. Leptin action in the dorsomedial hypothalamus increases sympathetic tone to brown adipose tissue in spite of systemic leptin resistance. Journal of Neuroscience 31:12189–12197.
[20] McMinn, J.E., Liu, S.M., Dragatsis, I., Dietrich, P., Ludwig, T., Eiden, S., et al., 2004. An allelic series for the leptin receptor gene generated by CRE and FLP recombinase. Mammalian Genome 15:677–685.
[21] van de Wall, E., Leshan, R., Xu, A.W., Balthasar, N., Coppari, R., Liu, S.M., et al., 2008. Collective and individual functions of leptin receptor modulated neurons controlling metabolism and ingestion. Endocrinology 149:1773–1785.
[22] Leshan, R.L., Bjornholm, M., Munzberg, H., Myers Jr., M.G., 2006. Leptin receptor signaling and action in the central nervous system. Obesity (Silver Spring) 14(Suppl. 5):208S–212S.
[23] Faouzi, M., Leshan, R., Bjornholm, M., Hennessey, T., Jones, J., Munzberg, H., 2007. Differential accessibility of circulating leptin to individual hypothalamic sites. Endocrinology 148:5414–5423.
[24] Paxinos, G., Franklin, K.B.J., 2004. The mouse brain in stereotaxic coordinates, Compact 2nd ed. Amsterdam; Boston: Elsevier Academic Press.
[25] Laque, A., Zhang, Y., Gettys, S., Nguyen, T.A., Bui, K., Morrison, C.D., et al., 2013. Leptin receptor neurons in the mouse hypothalamus are colocalized with the neuropeptide galanin and mediate anorexigenic leptin action. American Journal of Physiology. Endocrinology and Metabolism 304:E999–E1011.
[26] Gao, H., Miyata, K., Bhaskaran, M.D., Derbenev, A.V., Zsombok, A., 2012. Transient receptor potential vanilloid type 1-dependent regulation of liver-related neurons in the paraventricular nucleus of the hypothalamus diminished in the type 1 diabetic mouse. Diabetes 61:1381–1390.
[27] Jiang, Y., Gao, H., Krantz, A.M., Derbenev, A.V., Zsombok, A., 2013. Reduced GABAergic inhibition of kidney-related PVN neurons in streptozotocin-treated type 1 diabetic mouse. Journal of Neurophysiology 110:2192–2202.
[28] Nakamura, Y., Nakamura, K., Matsumura, K., Kobayashi, S., Kaneko, T., Morrison, S.F., 2005. Direct pyrogenic input from prostaglandin EP3 receptor-expressing preoptic neurons to the dorsomedial hypothalamus. European Journal of Neuroscience 22:3137–3146.
[29] Zaretskaia, M.V., Zaretsky, D.V., Sarkar, S., Shekhar, A., DiMicco, J.A., 2008. Induction of Fos-immunoreactivity in the rat brain following disinhibition of the dorsomedial hypothalamus. Brain Research 1200:39–50.
[30] Alexander, G.M., Rogan, S.C., Abbas, A.I., Armbruster, B.N., Pei, Y., Allen, J.A., et al., 2009. Remote control of neuronal activity in transgenic mice expressing evolved G protein-coupled receptors. Neuron 63:27–39.
[31] Krashes, M.J., Koda, S., Ye, C., Rogan, S.C., Adams, A.C., Cusher, D.S., et al., 2011. Rapid, reversible activation of AgRP neurons drives feeding behavior in mice. Journal of Clinical Investigation 121:1424–1428.
[32] Wulff, P., Arenkiel, B.R., 2012. Chemical genetics: receptor-ligand pairs for rapid manipulation of neuronal activity. Current Opinion in Neurobiology 22:54–60.
[33] Balthasar, N., Coppari, R., McMinn, J., Liu, S.M., Lee, C.E., Tang, V., et al., 2004. Leptin receptor signaling in POMC neurons is required for normal body weight homeostasis. Neuron 42:983–991.
[34] Coppari, R., Ichinose, M., Lee, C.E., Pullen, A.E., Kenny, C.D., McGovern, R.A., et al., 2005. The hypothalamic arcuate nucleus: a key site for mediating leptin's effects on glucose homeostasis and locomotor activity. Cell Metabolism 1:63–72.
[35] Dhillon, H., Zigman, J.M., Ye, C., Lee, C.E., McGovern, R.A., Tang, V., et al., 2006. Leptin directly activates SF1 neurons in the VMH, and this action by leptin is required for normal body-weight homeostasis. Neuron 49:191–203.
[36] Leinninger, G.M., Jo, Y.H., Leshan, R.L., Louis, G.W., Yang, H., Barrera, J.G., et al., 2009. Leptin acts via leptin receptor-expressing lateral hypothalamic neurons to modulate the mesolimbic dopamine system and suppress feeding. Cell Metabolism 10:89–98.
[37] Hommel, J.D., Trinko, R., Sears, R.M., Georgescu, D., Liu, Z.W., Gao, X.B., et al., 2006. Leptin receptor signaling in midbrain dopamine neurons regulates feeding. Neuron 51:801–810.
[38] Rothwell, N.J., Stock, M.J., 1983. Diet-induced thermogenesis. Advances in Nutritional Research 5:201–220.
[39] Nava, M.P., Abelenda, M., Puerta, M.L., 1990. Cold-induced and diet-induced thermogenesis in progesterone-treated rats. Pflugers Archiv 415:747–750.
[40] Himms-Hagen, J., 1989. Role of thermogenesis in the regulation of energy balance in relation to obesity. Canadian Journal of Physiology and Pharmacology 67:394–401.
[41] Crescenzo, R., Samec, S., Antic, V., Rohner-Jeanrenaud, F., Seydoux, J., Montani, J.P., et al., 2003. A role for suppressed thermogenesis favoring catch-up fat in the pathophysiology of catch-up growth. Diabetes 52:1090–1097.
[42] Harris, R.B., Zhou, J., Redmann Jr., S.M., Smagin, G.N., Smith, S.R., Rodgers, E., et al., 1998. A leptin dose-response study in obese (ob/ob) and lean (+/?) mice. Endocrinology 139:8–19.
[43] Pelleymounter, M.A., Cullen, M.J., Baker, M.B., Hecht, R., Winters, D., Boone, T., et al., 1995. Effects of the obese gene product on body weight regulation in ob/ob mice. Science 269:540–543.
[44] Doring, H., Schwarzer, K., Nuesslein-Hildesheim, B., Schmidt, I., 1998. Leptin selectively increases energy expenditure of food-restricted lean mice. International Journal of Obesity and Related Metabolic Disorders 22:83–88.
[45] Chao, P.T., Yang, L., Aja, S., Moran, T.H., Bi, S., 2011. Knockdown of NPY expression in the dorsomedial hypothalamus promotes development of brown adipocytes and prevents diet-induced obesity. Cell Metabolism 13:573–583.
[46] Bi, S., Kim, Y.J., Zheng, F., 2012. Dorsomedial hypothalamic NPY and energy balance control. Neuropeptides 46:309–314.
[47] Lee, S.J., Verma, S., Simonds, S.E., Kirigiti, M.A., Kievit, P., Lindsley, S.R., et al., 2013. Leptin stimulates neuropeptide Y and cocaine amphetamine-regulated transcript coexpressing neuronal activity in the dorsomedial

hypothalamus in diet-induced obese mice. Journal of Neuroscience 33: 15306–15317.

[48] Madden, C.J., Tupone, D., Morrison, S.F., 2012. Orexin modulates brown adipose tissue thermogenesis. Biomolecular Concepts 3:381–386.

[49] Tupone, D., Madden, C.J., Cano, G., Morrison, S.F., 2011. An orexinergic projection from perifornical hypothalamus to raphe pallidus increases rat brown adipose tissue thermogenesis. Journal of Neuroscience 31:15944–15955.

[50] Yamanaka, A., Beuckmann, C.T., Willie, J.T., Hara, J., Tsujino, N., Mieda, M., et al., 2003. Hypothalamic orexin neurons regulate arousal according to energy balance in mice. Neuron 38:701–713.

[51] Berglund, E.D., Liu, T., Kong, X., Sohn, J.W., Vong, L., Deng, Z., et al., 2014. Melanocortin 4 receptors in autonomic neurons regulate thermogenesis and glycemia. Nature Neuroscience 17:911–913.

[52] Kong, D., Tong, Q., Ye, C., Koda, S., Fuller, P.M., Krashes, M.J., et al., 2012. GABAergic RIP-Cre neurons in the arcuate nucleus selectively regulate energy expenditure. Cell 151:645–657.

[53] Hermann, G.E., Barnes, M.J., Rogers, R.C., 2006. Leptin and thyrotropin-releasing hormone: cooperative action in the hindbrain to activate brown adipose thermogenesis. Brain Research 1117:118–124.

[54] Harris, R.B., Kelso, E.W., Flatt, W.P., Bartness, T.J., Grill, H.J., 2006. Energy expenditure and body composition of chronically maintained decerebrate rats in the fed and fasted condition. Endocrinology 147:1365–1376.

[55] Barnes, M.J., Rogers, R.C., Van Meter, M.J., Hermann, G.E., 2010. Co-localization of TRHR1 and LepRb receptors on neurons in the hindbrain of the rat. Brain Research 1355:70–85.

[56] Rezai-Zadeh, K., Munzberg, H., 2013. Integration of sensory information via central thermoregulatory leptin targets. Physiology & Behavior 121:49–55.

[57] Bates, S.H., Dundon, T.A., Seifert, M., Carlson, M., Maratos-Flier, E., Myers Jr., M.G., 2004. LRb-STAT3 signaling is required for the neuroendocrine regulation of energy expenditure by leptin. Diabetes 53:3067–3073.

[58] Girardier, L., Clark, M.G., Seydoux, J., 1995. Thermogenesis associated with spontaneous activity: an important component of thermoregulatory needs in rats. Journal of Physiology 488(Pt 3):779–787.

[59] Nakamura, K., Morrison, S.F., 2011. Central efferent pathways for cold-defensive and febrile shivering. Journal of Physiology 589:3641–3658.

[60] Hunt, J.L., Zaretsky, D.V., Sarkar, S., Dimicco, J.A., 2010. Dorsomedial hypothalamus mediates autonomic, neuroendocrine, and locomotor responses evoked from the medial preoptic area. American Journal of Physiology – Regulatory, Integrative and Comparative Physiology 298:R130–R140.

[61] Babic, T., Purpera, M.N., Banfield, B.W., Berthoud, H.R., Morrison, C.D., 2010. Innervation of skeletal muscle by leptin receptor-containing neurons. Brain Research 1345:146–155.

[62] Bachman, E.S., Dhillon, H., Zhang, C.Y., Cinti, S., Bianco, A.C., Kobilka, B.K., et al., 2002. betaAR signaling required for diet-induced thermogenesis and obesity resistance. Science 297:843–845.

[63] Lecoultre, V., Ravussin, E., Redman, L.M., 2011. The fall in leptin concentration is a major determinant of the metabolic adaptation induced by caloric restriction independently of the changes in leptin circadian rhythms. Journal of Clinical Endocrinology and Metabolism 96:E1512–E1516.

